

1 **Multi-isotope labelling of organic matter by diffusion**
2 **of $^2\text{H}/^{18}\text{O}$ -vapour and $^{13}\text{C}\text{-CO}_2$ into the leaves and its**
3 **distribution within the plant**

4 **M. S. Studer^{1,2}, R. T. W. Siegwolf², M. Leuenberger³, S. Abiven¹**

5 [1] Department of Geography, University of Zurich, Winterthurerstr. 190, 8057
6 Zurich, Switzerland

7 [2] Laboratory of Atmospheric Chemistry, Paul Scherrer Institute, 5232 Villigen PSI,
8 Switzerland

9 [3] Climate and Environmental Physics, Physics Institute and Oeschger Centre for
10 Climate Change Research, University of Bern, Sidlerstr. 5, 3012 Bern

11 Correspondence to: Dr. S. Abiven (samuel.abiven@geo.uzh.ch)

12 **Abstract**

13 Isotope labelling is a powerful tool to study elemental cycling within terrestrial
14 ecosystems. Here we describe a new multi-isotope technique to label organic matter
15 (OM).

16 We exposed poplars (*Populus deltoides x nigra*) for 14 days to an atmosphere
17 enriched in $^{13}\text{CO}_2$ and depleted in $^2\text{H}_2^{18}\text{O}$. After one week, the water-soluble leaf OM
18 ($\delta^{13}\text{C} = 1346 \pm 162 \text{ ‰}$) and the leaf water were strongly labelled ($\delta^{18}\text{O} = -63 \pm 8 \text{ ‰}$,
19 $\delta^2\text{H} = -156 \pm 15 \text{ ‰}$). The leaf water isotopic composition was between the
20 atmospheric and stem water, indicating a considerable back-diffusion of vapour into
21 the leaves (58 - 69 %) in opposite direction to the net transpiration flow that itself is
22 reflected by the stem water resembling soil water composition. The atomic ratios of
23 the labels recovered ($^{18}\text{O}/^{13}\text{C}$, $^2\text{H}/^{13}\text{C}$) were 2 - 4 times higher in leaves than in the
24 stems and roots. This either indicates the synthesis of more condensed compounds
25 (lignin vs. cellulose) in roots and stems, or be the result of O and H exchange and
26 fractionation processes during transport and biosynthesis.

27 We demonstrate that the three major OM elements (C, O, H) can be labelled and
28 traced simultaneously within the plant. This approach could be of interdisciplinary
29 interest for the fields of plant physiology, paleoclimatic reconstruction or soil science.

30

31 **1 Introduction**

32 Artificial labelling with stable isotopes facilitates the observation of bio(geo)chemical
33 cycling of elements or compounds with minor disturbance to the plant-soil systems. It
34 has provided many insights into plant carbon allocation patterns (e.g. Simard et al.
35 1997; Keel et al. 2006; Högberg et al. 2008), water dynamics (e.g. in Plamboeck et al.
36 2007; Kulmatiski et al. 2010) and soil organic matter processes (e.g. in Bird and Torn
37 2006; Girardin et al. 2009) in terrestrial ecosystems. Only a few studies used labelling
38 approaches with more than one stable isotope, for example to study the interactions
39 between the carbon and nitrogen cycle (e.g. in Bird and Torn 2006; Schenck zu
40 Schweinsberg-Mickan et al. 2010). However, to our knowledge isotopic labelling of
41 organic matter (OM) with its three major elements, carbon (C), oxygen (O) and
42 hydrogen (H), has never been done in ecosystem studies before, even though
43 combined $\delta^{13}\text{C}$, $\delta^{18}\text{O}$ and $\delta^2\text{H}$ analyses have been widely used to study plant
44 physiological processes and to reconstruct past climatic conditions (Hangartner et al.,
45 2012; Roden and Farquhar, 2012; Scheidegger et al., 2000; Werner et al., 2012).
46 Similarly, an artificial labelling with those isotopes would be useful to clarify basic
47 mechanisms related to the plant water-use efficiency or the oxygen and hydrogen
48 signals in tree rings, but also to study other OM dynamics in the plant-soil system
49 such as OM decomposition in the soil.

50 The C, O and H contents of organic matter have been applied to distinguish major
51 groups of compounds, by plotting the atomic ratios O/C and H/C in a van Krevelen
52 diagram (Kim et al., 2003; Ohno et al., 2010; Sleighter and Hatcher, 2007). This
53 approach is based on the distinct molecular composition of organic compounds. For
54 example the glucose molecule ($\text{C}_6\text{H}_{12}\text{O}_6$) is characterized by high O/C (= 1) and H/C
55 (= 2) ratios and is the precursor of other compounds, such as cellulose ($(\text{C}_6\text{H}_{10}\text{O}_5)_{[n]}$)
56 O/C = 0.8, H/C = 1.7, Fig. 3a). Condensation or reduction reactions during
57 biosynthesis lead to other compound groups with lower atomic ratios (e.g. lignin) or
58 similar H/C, but lower O/C ratios (e.g. lipids, proteins) compared to glucose.
59 Following the logic of the van Krevelen diagram, we wanted to test, if we can use the
60 isotopic ratios $^{18}\text{O}/^{13}\text{C}$ and $^2\text{H}/^{13}\text{C}$ of the labels recovered in plant-soil bulk materials
61 after labelling the fresh assimilates with those stable isotopes, to detect the utilization
62 of the labelled assimilates for the synthesis of different OM compounds. With this
63 multi-labelling approach we would gain information about the characteristics of the

64 OM formed by simple isotopic analysis of bulk material. This has several advantages
65 compared to compound specific analysis, such as being much less laborious and less
66 expensive and yield integrated information on the bulk organic matter sampled.

67 In this study we added the ^{13}C , ^{18}O and ^2H labels via the gaseous phase in the plants'
68 atmosphere (CO_2 , water vapour). Pre-grown plants were exposed to the labelled
69 atmosphere continuously for fourteen days under laboratory conditions and the labels
70 added were traced in different plant compartments (leaves, petioles, new stems, stem
71 cuttings, roots) and soil organic matter at different points in time. We applied a simple
72 isotope mixing model to estimate the fraction of ^{18}O and ^2H that entered the leaf by
73 diffusion from the atmosphere into the leaf intercellular cavities and plotted the
74 atomic and isotopic ratios of the OM formed in van Krevelen diagrams to test if the
75 multi-isotope labelling approach can be used to detect changes in the OM
76 characteristics.

77 **2 Material and Methods**

78 **2.1 Plants and soil**

79 The soil (cambisol) was sampled from the upper 15 cm in a beech forest ($8^\circ 33' \text{ E}$, 47°
80 $23' \text{ N}$, 500 m elevation), coarse sieved (2.5 x 3.5 cm) and large pieces of hardly
81 decomposed organic material were removed. The soil had a clay loam texture, a pH of
82 4.8, an organic C content of 2.8 % and a C/N ratio of 11. The plant pots (volume = 8.2
83 dm^3) were filled with 3018 ± 177 g soil (dry weight equivalent). 15 Poplar seedlings
84 (*Populus deltoides x nigra*, Dorskamp clone) were grown indoors from 20 cm long
85 stem cuttings for five weeks before they were transferred into labelling chambers
86 (described below). They were kept in the chamber for acclimatization for one week
87 prior to labelling. At the beginning of the labelling experiments, the average dry
88 weight of fresh plant biomass (without the original stem cutting) was 3.3 ± 0.1 g and
89 the average total leaf area was 641 ± 6 cm^2 per plant. At the end of the experiment
90 (last sampling) the dry weight was 5.4 ± 1.1 g and the total leaf area was 1354 ± 161
91 cm^2 . The leaf area was measured with a handheld area meter (CID-203 Laser leaf area
92 meter, CID Inc.).

93 **2.2 Labelling chamber, procedure and environmental conditions**

94 The labelling chambers (MICE - Multi-Isotope labelling in a Controlled Environment
95 - facility) provide a hermetical separation of the shoots (leaves, petioles and new

96 stems) from the roots, rhizosphere and the soil. The plant shoots are enclosed by one
97 large polycarbonate cuboid (volume 1.2 m³) with a removable front plate and five 2
98 cm wide gaps in the bottom plate to slide in three plants in each row. Small
99 polycarbonate pieces, Kapton tape and a malleable sealant (Terostat IX, Henkel AG &
100 Co.) wrapped around the stem cuttings were used to seal off the upper from the lower
101 chamber. The belowground compartments (soil and roots) are in fifteen individual
102 pots, which are hermetically sealed from the laboratory and aerated with outdoor air.
103 This setup ensures that all plants receive the same labelling treatment and prevents the
104 diffusion of labelled atmospheric gases into the soil.

105 The environmental conditions in the MICE facility are automatically controlled and
106 monitored by a software (programmed with LabVIEW, National Instruments
107 Switzerland Corp.) switching on/off the light sources (Xenon, HELLA KGaA Hueck &
108 Co) and valves to in- or exclude instruments to regulate the CO₂ and H₂O
109 concentration, which is measured by an infrared gas analyzer (LI-840, LI-COR Inc.).
110 The chamber air is fed by a vacuum pump (N 815, KNF Neuberger AG) through
111 perforated glass tubes within a water reservoir to humidify the air or through a Peltier
112 cooled water condenser to dry the air (Appendix Fig. A1). Further the chamber air can
113 be fed through a Plexiglas tube filled with Soda lime to absorb the CO₂ or CO₂ is
114 injected from a gas cylinder.

115 The isotope labels (¹³C, ¹⁸O and ²H) were added continuously for 14 days via gaseous
116 phase to the plant shoots. We used CO₂ enriched in ¹³C (10 atom% ¹³C-CO₂,
117 Cambridge Isotope Laboratories, Inc.), and water vapour depleted in ¹⁸O and ²H ($\delta^{18}\text{O}$
118 = - 370 ‰ and $\delta^2\text{H}$ = - 813 ‰, waste product from enrichment columns at the Paul
119 Scherrer Institute). Thus the labelled gases added were enriched by 8.90 atom% ¹³C
120 and depleted by 0.07 atom% ¹⁸O and 0.01 atom% ²H relative to the ambient air.

121 The soil moisture was maintained at 100 % field capacity and the relative air humidity
122 was 74 %, in order to promote the back-diffusion of water into the leaves. The light
123 intensity was low ($80 \pm 25 \mu\text{mol m}^{-2} \text{s}^{-1}$ photosynthetic active radiation), and the CO₂
124 concentration was kept at 508 ± 22 ppm in order to maintain a high atmospheric
125 carbon supply. The day-night cycles were twelve hours and the temperature within the
126 labelling chamber was 31 ± 3 °C throughout the experiments.

127 **2.3 Sample collection**

128 The plant-soil systems were destructively harvested at five sampling dates (three
129 replicates each) to detect the dynamics of the labelling over time,. The first sampling
130 was done one day before the labelling experiment started (unlabelled control, referred
131 to as $t = 0$). Subsequently plant-soil systems were sampled after 1, 2, 8 and 14 days of
132 continuous labelling.

133 At each sampling date the plant-soil systems were separated into leaves, petioles,
134 stems, cuttings, roots (washed with deionised water and carefully dabbed with tissue)
135 and bulk soil (visible roots were removed with tweezers). The leaves (sub-sample of
136 six leaves) were sampled all along the stem (homogeneously distributed). The
137 uppermost leaves, newly formed during the experiment (completely labelled), were
138 excluded, since we wanted to study the tracer uptake and translocation dynamics in
139 already existing leaves prior to the treatment. In one out of the three plant replicates
140 we took two leaf sub-samples from distinct positions along the shoot. We sampled six
141 leaves from the upper and six leaves from the lower half of the shoot (thereafter
142 referred to as "top" and "bottom", respectively). Leaves, stems, roots and bulk soil
143 were collected in airtight glass vials and frozen immediately at $-20\text{ }^{\circ}\text{C}$ for later
144 cryogenic vacuum extraction of the tissue water. Cuttings and petioles were dried for
145 24 hours at $60\text{ }^{\circ}\text{C}$.

146 The tissue water was extracted with cryogenic vacuum extraction by heating the
147 frozen samples within the sampling vials in a water bath at $80\text{ }^{\circ}\text{C}$ under a vacuum
148 (10^{-3} mbar) for two hours. The evaporating water was collected in U-vials submersed
149 in a liquid nitrogen cold trap. After thawing (within the closed U-vials), the water
150 samples were transferred into vials and stored frozen at $-20\text{ }^{\circ}\text{C}$ for later $\delta^{18}\text{O}$ and $\delta^2\text{H}$
151 analysis. To study the water dynamics, additional water vapour samples from the
152 chamber air were collected by peltier-cooled water condensers (in an external air
153 circuit connected to the plant labelling chamber) and analysed for $\delta^{18}\text{O}$ and $\delta^2\text{H}$.

154 The dried plant residues of the cryogenic vacuum extraction were used for isotopic
155 bulk analyses (described below). The leaf water-soluble organic matter was extracted
156 by hot water extraction. 60 mg milled leaf material was dissolved in 1.5 ml of
157 deionised water and heated in a water bath ($85\text{ }^{\circ}\text{C}$) for 30 min. After cooling and
158 centrifugation ($10'000\text{ g}$, 2 min), the supernatant was freeze-dried and analysed for

159 $\delta^{13}\text{C}$. $\delta^2\text{H}$ analyses were not possible on the hot water extracts (mainly sugars), due to
160 incomplete equilibration with ambient water vapour (Filot, 2010).

161 **2.4 Isotopic and elemental analyses**

162 All samples were milled to a fine powder with a steel ball mill and weighed into tin
163 ($\delta^{13}\text{C}$ analyses) or silver ($\delta^{18}\text{O}$ and $\delta^2\text{H}$ analyses) capsules and measured by isotope-
164 ratio mass spectrometry (IRMS). The $\delta^{13}\text{C}$ samples were combusted at 1700 °C in an
165 elemental analyser (EA 1110, Carlo Erba) and the resulting CO_2 was transferred in a
166 helium stream via a variable open-split interface (ConFlo II, Finnigan MAT) to the
167 IRMS (Delta S, Thermo Finnigan; see Werner et al. 1999). The samples for $\delta^{18}\text{O}$
168 analyses were pyrolysed at 1040 °C in an elemental analyser (EA 1108, Carlo Erba)
169 and transferred via ConFlo III interface (Thermo Finnigan) to the IRMS (Delta plus
170 XL, Thermo Finnigan). The samples for $\delta^2\text{H}$ analyses were equilibrated with water
171 vapour of known signature prior to the IRMS measurements, to determine the isotopic
172 signature of the non-exchangeable hydrogen (as described in Filot et al. 2006;
173 Hangartner et al. 2012). After equilibration the samples were pyrolysed in a
174 thermochemical elemental analyser (TC/EA, Thermo-Finnigan) at a temperature of
175 1425 °C and the gaseous products were carried by a helium stream via a ConFlow II
176 open split interface (Thermo Finnigan) into the IRMS (Isoprime, Cheadle). The
177 amount of exchangeable hydrogen (25-27%) and oxygen (2-3%) was measured for
178 the leaf, stem and root tissue using depleted water vapour to equilibrate the samples.
179 The measurement precisions of the solid sample analyses were 0.12 ‰ $\delta^{13}\text{C}$, 0.54 ‰
180 $\delta^{18}\text{O}$ and 1 ‰ $\delta^2\text{H}$ and were assessed by working standards measured frequently
181 along with the experimental samples. The precisions were lower than reported for
182 measurements of natural abundance, since highly labelled sample material was
183 analysed.

184 Elemental C, H and N content of solid samples was analysed in an elemental analyzer
185 (CHN-900, Leco Corp.) and the elemental O content by RO-478 (Leco Corp.).

186 The liquid samples from the cryogenic vacuum extraction (tissue water) were
187 pyrolysed in an elemental analyser (TC/EA, Thermo Finnigan) and the evolving CO
188 and H_2 gases were transferred via the ConFlo III interface (Thermo Finnigan) to a
189 IRMS (Delta plus XL, Thermo Finnigan) for oxygen and hydrogen isotope ratio
190 analysis (Gehre et al., 2004). The precision of the liquid sample measurement was \pm
191 0.75 ‰ $\delta^{18}\text{O}$ and \pm 1.59 ‰ $\delta^2\text{H}$.

192 **2.5 Calculations**

193 Isotopic ratios were expressed in delta (δ) notation as the deviation (in ‰) from the
 194 international standards Vienna Pee Dee Belemnite (V-PDB, $^{13}\text{C}/^{12}\text{C} = 1.11802 \times 10^{-2}$)
 195 and Vienna Standard Mean Ocean Water (V-SMOW, $^{18}\text{O}/^{16}\text{O} = 2.0052 \times 10^{-3}$ and
 196 $^2\text{H}/^1\text{H} = 1.5575 \times 10^{-4}$). The significance of changes in isotopic signature between the
 197 sampling dates and the unlabelled control ($t = 0$) were statistically tested by t-tests
 198 performed by R software (R Core Team 2014).

199 In the following paragraphs we describe first the calculations for the leaf water source
 200 partitioning (Eqs. 1 - 4). These equations are given for the oxygen isotope (^{18}O), but
 201 they apply also for hydrogen (^2H). Then we describe the calculations for the relative
 202 recovery of the isotopes ($^{18}\text{O}/^{13}\text{C}$ and $^2\text{H}/^{13}\text{C}$) in the bulk organic matter (Eqs. 5 - 7).

203 The leaf water isotopic signature (at steady state) can be described by a model of
 204 Dongmann et al. (1974) to calculate leaf water H_2^{18}O enrichment, a derivative of
 205 Craig & Gordon (1965) (Eq. 1). According to this model, the isotopic signature of the
 206 leaf water (L) is the result of kinetic (ϵ^k) and equilibrium (ϵ^*) fractionation processes
 207 during evaporation of the source water (S) within the leaves and the back-diffusion of
 208 atmospheric water vapour (V) into the leaves as affected by relative air humidity (h).

209
$$\delta^{18}\text{O}_L = \delta^{18}\text{O}_S + \epsilon^k + \epsilon^* + (\delta^{18}\text{O}_V - \delta^{18}\text{O}_S - \epsilon^k) \cdot h \quad (1)$$

210 We used a two-source isotope mixing model (Eq. 2, principles described in Dawson et
 211 al. 2002) to assess the contribution of the two main water pools (soil and atmospheric
 212 water) to the leaf water based on its isotopic signatures. An overview on the input data
 213 for the mixing model is given as in Appendix A (Fig. A1).

214
$$f_{source,2} = \frac{\delta^{18}\text{O}_{leaf,water} - \delta^{18}\text{O}_{source,1}}{\delta^{18}\text{O}_{source,2} - \delta^{18}\text{O}_{source,1}} \quad (2)$$

215 , where $\delta^{18}\text{O}_{leaf,water}$ is the isotopic signature (in ‰) of water extracted from the leaves
 216 at a specific sampling date and $\delta^{18}\text{O}_{source,1}$ and $\delta^{18}\text{O}_{source,2}$ are the theoretical isotopic
 217 signatures of the leaf water if all water would originate either from the soil (source 1)
 218 or the atmospheric (source 2) water pool.

219 The first source, thereafter referred to as "evaporating source", represents the water
 220 taken up from the soil by the roots, which is transported via the xylem to the leaf,
 221 where it evaporates. The isotopic signature of the evaporating source (Eq. 3) is

222 estimated by the maximum leaf water enrichment that would occur at 0 % relative air
 223 humidity i.e. by the first part of the Dongmann approach (solving Eq. 1 with $h = 0$).

$$224 \quad \delta^{18}\text{O}_{source,1} = \delta^{18}\text{O}_{stem,water} + \epsilon^k + \epsilon_{atm}^* \quad (3)$$

225 , where $\delta^{18}\text{O}_{stem,water}$ is the isotopic signature (in ‰) of the water extracted from the
 226 stem tissue (approximating the xylem water) and ϵ^k and ϵ_{atm}^* are the kinetic and
 227 equilibrium fractionation terms, respectively, at the specific sampling date.

228 The second source, thereafter called "condensation source", refers to the water vapour
 229 that diffuses from the atmosphere into the leaves and condensates at the cell walls.
 230 The contribution of this source would be maximal at 100 % relative humidity, which
 231 results in Eq. 4 when solving Eq. 1 with $h = 1$.

$$232 \quad \delta^{18}\text{O}_{source,2} = \delta^{18}\text{O}_{atm,vap} + \epsilon_{atm}^* = \delta^{18}\text{O}_{atm,cond} - \epsilon_{pelt}^* + \epsilon_{atm}^* \quad (4)$$

233 , where $\delta^{18}\text{O}_{atm,vap}$ is the isotopic signature of the water vapour of the chamber
 234 atmosphere and ϵ_{atm}^* is the equilibrium fractionation inside the chamber at the specific
 235 sampling date. The signature of the atmospheric water vapour was measured on its
 236 condensate ($\delta^{18}\text{O}_{atm,cond}$) collected in the peltier water trap, which was therefore
 237 corrected with the equilibrium fractionation during condensation inside the peltier-
 238 cooled water condenser (ϵ_{pelt}^*).

239 The kinetic fractionation due to the difference in molecular diffusivity of the water
 240 molecule species ($\epsilon^k = 20.7$ ‰ $\delta^{18}\text{O}$ and 10.8 ‰ $\delta^2\text{H}$) was estimated according to
 241 Cappa et al. (2003) for a laminar boundary layer (Schmidt-number $q = 2/3$,
 242 Dongmann et al. 1974). The equilibrium fractionation due to the phase change during
 243 evaporation and condensation at different temperatures was calculated as in Majoube
 244 (1971) with the conditions present at the specific day. The condensation (dew point)
 245 temperature inside the peltier-cooled water condenser ($T_{pelt,DP}$) was determined based
 246 on the remaining humidity and the air pressure of the air leaving the condenser
 247 (details on the calculation are given in Appendix B). The equilibrium fractionation
 248 factors during the labelling experiment were on average $\epsilon_{atm}^* = 8.9 \pm 0.2$ ‰ for $\delta^{18}\text{O}$
 249 and 72.7 ± 2.7 ‰ for $\delta^2\text{H}$ at $T = 31.3 \pm 2.7$ °C inside the labelling chamber and $\epsilon_{pelt}^* =$
 250 11.1 ± 0.2 ‰ for $\delta^{18}\text{O}$ and 103.3 ± 3.3 ‰ for $\delta^2\text{H}$ at $T_{pelt,DP} = 6.0 \pm 2.5$ °C inside the
 251 water condenser.

252 We compared the distribution of the assimilated labels (^{13}C , ^{18}O , ^2H) in the leaf, stem
 253 and root tissue by its isotopic ratios. Therefore we converted the δ -notation to atom
 254 fraction (Eq. 5) according to Coplen (2011).

$$255 \quad x(^{13}\text{C})_{t=x} = \frac{1}{1 + \frac{1}{(\delta^{13}\text{C}_{t=x}/1000 + 1) \cdot R_{V-PDB}}} \quad (5)$$

256 , where $\delta^{13}\text{C}_{t=x}$ is the isotopic signature (in ‰) of the bulk tissue at sampling date x
 257 and R is the ratio of the heavier to the lighter isotope ($^{13}\text{C}/^{12}\text{C}$) of the international
 258 standard V-PDB. The atom fraction of ^{18}O and ^2H was calculated accordingly, but
 259 using R_{V-SMOW} as reference and neglecting the ^{17}O isotope amount.

260 For the Van Krevelen approach we calculated the elemental ratios. The relative
 261 label distribution ($^{18}\text{O}/^{13}\text{C}$ and $^2\text{H}/^{13}\text{C}$) within the plant organic matter (OM) was
 262 calculated based on the excess atom fraction measured in each tissue (Eq. 6).

$$263 \quad \frac{x^E(^{18}\text{O}_{tissue,OM})_{t=x/t=0}}{x^E(^{13}\text{C}_{tissue,OM})_{t=x/t=0}} = \frac{x(^{18}\text{O}_{tissue,OM})_{t=x} - x(^{18}\text{O}_{tissue,OM})_{t=0}}{x(^{13}\text{C}_{tissue,OM})_{t=x} - x(^{13}\text{C}_{tissue,OM})_{t=0}} \quad (6)$$

264 , where $x^E(^{18}\text{O})_{t=x/t=0}$ and $x^E(^{13}\text{C})_{t=x/t=0}$ is the excess atom fraction of the labels detected
 265 at a specific sampling date ($t = x$), relative to the unlabelled control ($t = 0$). Eq. 6 and
 266 7 was analogously calculated for the $^2\text{H}/^{13}\text{C}$ ratio.

267 In a second step we corrected the isotopic ratios ($^{18}\text{O}/^{13}\text{C}$ and $^2\text{H}/^{13}\text{C}$) with the
 268 maximum label strength of the precursor of the organic matter, i.e. the maximum label
 269 strength of fresh assimilates (Eq. 7), which was assumed to be the excess atom
 270 fraction of ^{13}C in the leaf water-soluble organic matter (wsOM) and the excess atom
 271 fraction of ^{18}O and ^2H in the leaf water (relative to the unlabelled control).

$$272 \quad \frac{x^E_{norm}(^{18}\text{O}_{tissue,OM})_{t=x/t=0}}{x^E_{norm}(^{13}\text{C}_{tissue,OM})_{t=x/t=0}} = \frac{x^E(^{18}\text{O}_{tissue,OM})_{t=x/t=0}}{x^E(^{13}\text{C}_{tissue,OM})_{t=x/t=0}} \cdot \frac{x^E(^{13}\text{C}_{leaf,wsOM})_{t=x/t=0}}{x^E(^{18}\text{O}_{leaf,water})_{t=x/t=0}} \quad (7)$$

273 3 Results

274 3.1 Labelling of the leaf water and water-soluble OM

275 The ^{18}O and ^2H label added as water vapour to the chamber atmosphere ($\delta^{18}\text{O} = - 370$
 276 ‰, $\delta^2\text{H} = - 813$ ‰), was mixed with transpired water, which was isotopically
 277 enriched compared to the added label (Fig. 1). The isotopic signature of the water

278 vapour within the chamber air stabilized after four days at a level of $-112 \pm 4 \text{ ‰ } \delta^{18}\text{O}$
279 and $-355 \pm 7 \text{ ‰ } \delta^2\text{H}$. Thus the atmospheric water vapour signature was depleted in
280 ^{18}O by $94 \pm 4 \text{ ‰}$ and in ^2H by $183 \pm 7 \text{ ‰}$ compared to the unlabelled atmosphere.

281 The leaf water was strongly depleted and its isotopic signature was stable at a level of
282 $-64 \pm 7 \text{ ‰}$ for $\delta^{18}\text{O}$ and $-158 \pm 13 \text{ ‰}$ for $\delta^2\text{H}$ already after two days of labelling with
283 the depleted water vapour (Fig. 1). The leaf water was thus on average depleted by 63
284 $\pm 7 \text{ ‰}$ for $\delta^{18}\text{O}$ and $126 \pm 14 \text{ ‰}$ for $\delta^2\text{H}$ compared to the unlabelled leaf water
285 signature and it was between the signature of the atmospheric water vapour and the
286 water added to the soil ($\delta^{18}\text{O} = -9 \pm 0 \text{ ‰}$, $\delta^2\text{H} = -74 \pm 2 \text{ ‰}$). This indicates that a
287 substantial amount of the leaf water originated from the atmospheric water pool,
288 suggesting that it entered the leaf via diffusion through the stomata. The depletion of
289 the water within a leaf was dependent on its position on the shoot (Fig. 2c,e). The leaf
290 water of the leaves sampled in the upper half of the shoot was $7 \pm 2 \text{ ‰}$ and $18 \pm 8 \text{ ‰}$
291 less depleted in $\delta^{18}\text{O}$ and $\delta^2\text{H}$ than the leaves sampled at the lower half. The isotopic
292 signature of the stem water ($\delta^{18}\text{O} = -10 \pm 0 \text{ ‰}$ and $\delta^2\text{H} = -74 \pm 4 \text{ ‰}$), as well as the
293 root ($\delta^{18}\text{O} = -6 \pm 1 \text{ ‰}$ and $\delta^2\text{H} = -58 \pm 4 \text{ ‰}$) and the soil water ($\delta^{18}\text{O} = -6 \pm 1 \text{ ‰}$
294 and $\delta^2\text{H} = -63 \pm 3 \text{ ‰}$), was not significantly depleted and reflected the signature of
295 the water added to the soil (Fig. 1).

296 At the second sampling date, the leaf water seemed to be more depleted than the water
297 vapour within the chamber air (Fig. 1). This is the result of different sampling
298 procedures. The leaf sampling was performed at one point in time (three hours after
299 the light switched on), while the atmospheric water vapour collected by condensation
300 represents an average on the previous 24 hours. Therefore the depletion of the water
301 vapour is underestimated before the equilibrium of the isotopic signature in the
302 atmosphere was reached. In the following the average values of signatures detected
303 after the equilibrium was reached are given ($t = 8$ and $t = 14$). We tried to estimate the
304 contribution of the isotopic signature of the atmospheric water vapour that enters the
305 leaf by diffusion with a two-source mixing model (Tab. 1). The results were obtained
306 by the two water isotopes ^{18}O and ^2H separately. Both indicated a substantial
307 contribution of the atmospheric water vapour to the leaf water isotopic signature,
308 whereby the estimates based on the oxygen isotope yielded a higher contribution (69
309 $\pm 7 \text{ ‰}$) than the hydrogen estimates ($58 \pm 4 \text{ ‰}$). The estimates for the leaves sampled
310 at different position on the shoot varied by 5 ‰ , whereas the contribution of
311 atmospheric water to the leaf water was higher in the leaves sampled at the bottom

312 (71 ± 4 ‰ based on ¹⁸O and 60 ± 2 ‰ based on ²H) than in the leaves at the top (66 ±
313 2 ‰ and 55 ± 0 ‰, respectively) of the shoots.

314 The ¹³C-CO₂ added (8938 ‰ δ¹³C) was assumingly also strongly diluted by respired
315 ¹²C-CO₂, but we did not measure the isotopic signature of the CO₂ within the chamber
316 air. The leaf water-soluble OM was significantly enriched already after one day of
317 labelling and levelled off towards the end of the experiment. At the last two sampling
318 dates its isotopic signature was on average 1346 ± 162 ‰ δ¹³C.

319 **3.2 Labelling of the bulk organic matter**

320 All three applied labels could be detected in the plant bulk material (Tab. 2). We
321 measured the isotopic signature of the non-exchangeable hydrogen, which was
322 estimated to be 74 ± 1 ‰ of the total OM. After fourteen days of continuous labelling,
323 the leaves, petioles, stems and roots were enriched by 650 - 1150 ‰ in δ¹³C, depleted
324 by 4 - 17 ‰ in δ¹⁸O and 6 - 31 ‰ in δ²H. Thus the plant biomass was significantly
325 labelled even under the extreme environmental conditions (high temperature and low
326 light availability) that were critical for net C assimilation (increasing tissue respiration
327 and reducing photosynthesis, respectively). However, the labelling was not strong
328 enough to trace the OM within the large OM pools of the cuttings and soil organic
329 matter, in which the change in isotopic signature was close to the detection limit or
330 could not be detected. The measured depletion in ¹⁸O of the bulk soil can be
331 accounted for natural variability, since the same effect has been observed in non-
332 treated soil (data not shown here).

333 The labelling of the leaf bulk OM occurred in parallel to the labelling of the leaf water
334 and water-soluble OM (Fig. 2). The leaf OM was enriched in ¹³C after one day (Fig.
335 2b) and depleted in ¹⁸O and ²H after two days (Fig. 2d,f). The incorporation of the
336 label into the leaf OM was, as the labelling of the leaf water, dependent on the
337 position on the shoot. The biomass of the leaves at the top was more enriched in ¹³C
338 (by up to 673 ‰) than the biomass of the leaves at the bottom of the shoots, and in
339 contrast to the leaf water, more depleted in ¹⁸O and ²H (by up to 9 and 21 ‰,
340 respectively) at the top than at the bottom. This indicates a higher overall assimilation
341 in the leaves at the top of the shoot.

342 **3.3 Atomic and isotopic ratios to characterize organic matter**

343 The atomic ratios of the plant bulk OM were in the range of 13.7 - 115.4 C/N, 0.70 -
344 0.83 O/C and 1.56 - 1.72 H/C (Tab. 3). The leaf OM was characterized by the lowest
345 C/N and O/C ratios and concurrently by highest H/C ratios (Fig. 3a). The other plant
346 tissues indicated a linear trend in decreasing O/C and H/C and increasing C/N ratios
347 in the order of stems, petioles, roots and cuttings.

348 The recovery of the three isotopes varied between the leaf, stem and root tissue, while
349 they were similar between the sampling dates (Fig. 3b). The isotopic ratios of the
350 excess atom fractions were $3.5 \pm 0.4 \times 10^{-3} \text{ }^{18}\text{O}/^{13}\text{C}$ and $5.3 \pm 0.5 \times 10^{-4} \text{ }^2\text{H}/^{13}\text{C}$ in the
351 leaves, $1.4 \pm 0.1 \times 10^{-3} \text{ }^{18}\text{O}/^{13}\text{C}$ and $2.9 \pm 0.6 \times 10^{-4} \text{ }^2\text{H}/^{13}\text{C}$ in the stems and $1.0 \pm 0.2 \times$
352 $10^{-3} \text{ }^{18}\text{O}/^{13}\text{C}$ and $1.0 \pm 1.4 \times 10^{-4} \text{ }^2\text{H}/^{13}\text{C}$ in the roots after the equilibrium in the leaf
353 water and water-soluble OM labelling was reached. Thus the $^{18}\text{O}/^{13}\text{C}$ ratios were on
354 average 2.6 (± 0.2) times lower in the stems and 3.8 (± 0.7) times lower in the roots
355 than in the leaves (Tab. 3) and the $^2\text{H}/^{13}\text{C}$ ratios 1.9 (± 0.2) and 3.1 (± 0.6) times lower
356 in the stems and roots, respectively, than in the leaves.

357 After correction for the maximum label strength (^{18}O , ^2H and ^{13}C excess atom fraction
358 within the leaf water and the water-soluble OM, respectively), the isotopic ratios were
359 in the range of 0.17 - 0.43 $^{18}\text{O}/^{13}\text{C}$ and 0.14 - 0.23 $^2\text{H}/^{13}\text{C}$. The normalized isotopic
360 ratios were thus in the magnitude order of the atomic ratios reported for OM
361 compounds (Tab. 3, Fig. 3c), however lower than expected for fresh organic matter
362 (in the range characteristic for condensed hydrocarbons).

363 **4 Discussion**

364 **4.1 Diffusion of atmospheric water vapour into the leaf**

365 The strong depletion in $\delta^{18}\text{O}$ and $\delta^2\text{H}$ observed in the leaf water indicates a high back-
366 diffusion of labelled water vapour from the atmosphere into the leaf. The diffusion is
367 dependent on the gradient between atmospheric and leaf water vapour pressure and
368 the stomatal conductance (Parkhurst, 1994). The higher the atmospheric water vapour
369 pressure (the smaller the gradient), the more water molecules diffuse back into the
370 leaf. The latter is further enhanced the larger the stomatal conductance is (Reynolds
371 Henne, 2007). Here we maintained the atmospheric vapour pressure constant at a high
372 level, ensuring a high back-diffusion at a given stomatal conductance. In our
373 experiment the leaf water $\delta^{18}\text{O}$ and $\delta^2\text{H}$ signature is determined by i) the signature and

374 the amount of labelled (depleted) water vapour diffusing into the leaf intercellular
375 cavities, ii) by the enrichment due to transpiration (kinetic and equilibrium
376 fractionation) and iii) by the influx of xylem water, which is isotopically enriched
377 relative to the labelled water vapour. The latter is proportionally enhanced by
378 increasing transpiration rates as a result of the diffusion convection process of H₂O
379 (Péclet effect, Farquhar and Lloyd 1993).

380 The distinct label signal in the water sampled in leaves at different positions on the
381 shoot indicates differences in the transpiration rate. Meinzer et al. (1997)
382 demonstrated in large poplar trees that shading or lower irradiance leads to lower
383 stomatal conductance and transpiration rates. Thus the back-diffusion in the leaves on
384 the bottom might have been reduced due to lower stomatal conductance. However, the
385 increased transpiration in the leaves at the top, lead to an even stronger dilution of the
386 isotopic signal in the leaf water due to i) increased evaporative leaf water enrichment
387 and ii) the Péclet effect (enhanced influx of xylem water, which was enriched
388 compared to the labelled atmospheric water vapour).

389 The amount of leaf water that entered the leaf by back-diffusion was estimated to be
390 58-69 %. This result is in contradiction to the common perception that most of the leaf
391 water is taken up from the soil via roots. However it is in line with the observations
392 made by Farquhar & Cernusak (2005), who modelled the leaf water isotopic
393 composition in the non-steady state and estimated the contribution of atmospheric
394 water to the leaf water to be approximately two-thirds of the total water supply.
395 Albeit, our estimates are based on a modelling approach that does not take into
396 account the Péclet effect or daily fluctuations in the isotopic signatures as described
397 below, our estimates correspond very well the findings of Farquhar & Cernusak
398 (2005).

399 The model used to estimate the quantitative contribution of the two water sources is
400 based on the measured signature of the leaf water ($\delta^{18}\text{O}_{\text{leaf,water}}$) and the estimated
401 signatures of the water at the evaporating and condensation site ($\delta^{18}\text{O}_{\text{source,1}}$ and
402 $\delta^{18}\text{O}_{\text{source,2}}$, respectively). The “dilution” of the (laminar) leaf water with the relatively
403 enriched xylem water through the Péclet effect is included in the $\delta^{18}\text{O}_{\text{leaf,water}}$. This
404 explains the lower contribution of atmospheric water (- 5 %) estimated in the leaves
405 sampled at the top (due to the Péclet effect resulting from higher transpiration rates)
406 compared to the leaves sampled at the bottom of the shoot.

407 Some inaccuracy in the two-source mixing model estimates might have been
408 introduced by daily fluctuations in the environmental and labelling conditions. The
409 mixture ($\delta^{18}\text{O}_{\text{leaf,water}}$) was sampled after three hours of light, whereas the estimation
410 of the two sources ($\delta^{18}\text{O}_{\text{source,1}}$ and $\delta^{18}\text{O}_{\text{source,2}}$) is based on daily average values of
411 environmental parameters and the atmospheric water vapour ($\delta^{18}\text{O}_{\text{atm,vap}}$) label
412 strength. In our experiment, fluctuations in $\delta^{18}\text{O}_{\text{atm,vap}}$ were caused by adding the
413 labelled vapour mainly during night-time, when transpiration was low. Thus the
414 atmospheric label strength was assumingly highest before the lights were switched on
415 and gradually diluted during the day by transpired water vapour. Hence the actual
416 $\delta^{18}\text{O}_{\text{atm,vap}}$ at the time of plant sampling was probably more depleted than the
417 measured average signature. Therefore $\delta^{18}\text{O}_{\text{source,2}}$ and its contribution to the leaf
418 water was slightly overestimated. The effect of the temperature fluctuations ($\pm 3\text{ }^\circ\text{C}$)
419 via changes in the equilibrium fractionation was minor for the outcome of the mixing
420 model $< 1\%$.

421 Nonetheless, the strong depletion of the leaf water in ^2H and ^{18}O proofs, that back-
422 diffusion of atmospheric water vapour into the leaf is an important mechanisms for
423 leaf water uptake. This supports the hypothesis that atmospheric water vapour
424 diffusion might be as important as the flux of water from the xylem into the leaf (at
425 least under humid conditions) and be an important mechanisms for the reversed water
426 flow observed in the tropics (Goldsmith, 2013). Furthermore, these results
427 demonstrate that the leaf water isotopic composition is strongly affected by the
428 atmospheric signature at humid conditions and that thus the applicability of the dual-
429 isotope approach (Scheidegger et al., 2000), e.g. to reconstruct past climate conditions
430 by tree ring analysis, is only valid if the source water and atmospheric vapour $\delta^{18}\text{O}$
431 are similar. The back-diffusion of atmospheric vapour at high humidity could be
432 another factor next to the evaporative enrichment (as demonstrated by Roden and
433 Farquhar, 2012) to overshadow the effects of stomatal conductance on the leaf $\delta^{18}\text{O}$
434 signature.

435 **4.2 Tracing organic matter?**

436 The O/C and H/C ratio of the plant bulk material was close to the signature of
437 cellulose (Fig. 3a). The leaves had a lower O/C ratio with a constant high H/C ratio
438 indicating that its OM contains more reduced compounds such as amino-sugars or
439 proteins, which is also supported by its low C/N ratio. The trend of decreasing O/C

440 and H/C ratios observed in the other tissues is in the direction of condensation
441 reactions. This trend most likely indicates the increasing lignification of OM from
442 shoots, to roots, to cuttings.

443 The same trend has been observed in the ratios of the labels added from the leaf, to
444 the stem, to the root OM (Fig. 3b,c). The lower isotopic O/C and H/C ratios in the
445 root and stem tissue compared to the leaf tissue could indicate the utilization of the
446 labelled assimilates for the synthesis of more condensed compounds (e.g. lignin) in
447 those tissues. However, other factors affecting the isotopic ratios of the OM are the
448 maximum label strength, the exchange of hydrogen and oxygen with xylem water
449 during transport and biosynthesis and the isotopic fractionation during metabolism.

450 The isotopic ratios (Fig. 3b) were around three magnitudes smaller than the expected
451 atomic ratios of OM (Sleighter and Hatcher, 2007). This is mainly due to the different
452 maximum label strength, which was highest for the ^{13}C and lowest for the ^2H . After
453 correction for this factor, the isotopic ratios were in the range of the atomic ratios
454 characteristic for condensed hydrocarbons (Fig. 3c). The isotopic ratios might be
455 lower than expected due to inaccurate approximation of the maximum label strength
456 of fresh assimilates (by the leaf water and water-soluble OM), or be the result of ^{18}O
457 and ^2H label losses during transport and biosynthesis.

458 One reason for the label loss might be the use of other (more enriched) sources during
459 biosynthesis. For example O_2 (enriched by 23 ‰ $\delta^{18}\text{O}$) has been identified as a further
460 source for aromatic compounds, such as phenols and sterols (Schmidt et al., 2001).
461 However, for hydrogen, water is the only known source (Schmidt et al., 2003) and
462 therefore the use of other O or H sources during biosynthesis can not explain the
463 (major) loss of the ^{18}O and ^2H label.

464 Another potential reason would be the kinetic fractionation during biosynthesis that
465 leads to distinct isotopic signatures of different OM compounds (described in Schmidt
466 et al. 2001, 2003; Badeck et al. 2005; Bowling et al. 2008). However, assuming
467 constant isotopic fractionation during the experimental period (constant
468 environmental conditions), the isotopic ratios would not be affected, since they are
469 based on the excess atom fraction relative to the unlabelled OM.

470 A third reason for the loss of the ^{18}O and ^2H label could be the exchange of hydrogen
471 and oxygen atoms with water. O and H exchanges with tissue water during transport
472 and the synthesis of new compounds (as recently discussed for oxygen in phloem
473 sugars and cellulose in Offermann et al. 2011 and Gessler et al. 2013). O of carbonyl

474 groups (Barbour, 2007; Sternberg et al., 1986) and H in nucleophilic OH and NH
475 groups or H adjacent to carbonyl groups (Augusti et al., 2006; Garcia-Martin et al.,
476 2001) exchange with water. Thus biochemical reactions lead to different isotopomers
477 of organic compounds (Augusti and Schleucher, 2007). The proportion of O and H
478 exchanged can be considerable, e.g. during cellulose synthesis around 40 % of O and
479 H are exchanged with the tissue water (Roden and Ehleringer, 1999; Yakir and
480 DeNiro, 1990). The exchange with water explains to some extent the stronger relative
481 ^{18}O and ^2H signal in the leaf OM compared to the stem and root OM, since the leaf
482 water was labelled, while the stem and root water was not. Especially the $^{18}\text{O}/^{13}\text{C}$
483 isotopic ratios were increased in the leaf OM compared to the relations observed in
484 the atomic ratios (Fig. 3a). The leaf OM has the lowest O/C atomic ratios while it has
485 the highest $^{18}\text{O}/^{13}\text{C}$ isotopic ratios of all plant compartments (Tab. 3). This effect is
486 less expressed for the $^2\text{H}/^{13}\text{C}$ ratios, since only the fraction of hydrogen that does not
487 exchange with ambient water vapour is measured. The non-exchangeable fraction (74
488 %) is hydrogen bound to carbon (Filot et al., 2006), which is hardly exchanged with
489 xylem water.

490 **5 Conclusions**

491 We present a new technique to label organic matter at its place of formation by the
492 application of labels through the gaseous phase ($^{13}\text{CO}_2$ and $^2\text{H}_2^{18}\text{O}$). In this study we
493 could show that in a humid atmosphere, the atmospheric water vapour isotopic
494 signature dominates the leaf water signature, due to a strong back-diffusion of water
495 vapour into the leaf. Further we detected differences in the relative distribution of ^{13}C ,
496 ^{18}O and ^2H in the leaves, stems and roots. This could indicate the synthesis of
497 different compounds in the particular tissues (change in OM characteristics), but it
498 could also be the result of exchange and fractionation processes during transport and
499 biosynthesis. To further test these two possibilities a better estimation of the
500 maximum label strength by compound specific sugar analysis would be needed,
501 which has been further developed for $\delta^{13}\text{C}$ (Rinne et al., 2012) and for $\delta^{18}\text{O}$ (Zech et
502 al., 2013) recently, but does not yet exist for $\delta^2\text{H}$ analysis.

503 The multi-isotope labelling technique can be used to assess the amount of vapour
504 diffusing into the leaves and to trace the dynamics of the labelled organic matter. It
505 could be applied in soil sciences, e.g. to track the decomposition pathways of soil OM
506 inputs, or in the field of plant physiology and paleoclimatic reconstruction, e.g. to

507 further investigate the O and H exchange and fractionation processes during transport
508 and metabolic processes or the importance of the ambient air humidity besides its
509 isotopic composition for the climate signal stored in tree-ring cellulose. Furthermore
510 the multi-isotope labelling technique has the potential to make changes of OM
511 characteristics visible (e.g. C allocation into the non-structural vs. structural pool), for
512 example after a change in climatic conditions, and to trace the labelled OM during its
513 decomposition within the soil.

514 **Acknowledgements**

515 This study was funded by the Swiss National Science Foundation (SNSF), project
516 number 135233. We would like to thank Professor M. W. I Schmidt for his support,
517 M. Saurer for his comments on the manuscript, R. Künzli, I. Lötscher, R. Maier, P.
518 Nyfeler and I. Woodhatch for technical assistance, and the soil science and
519 biogeochemistry (University of Zurich) and the ecosystem fluxes (Paul Scherrer
520 Institute) research groups for valuable discussions.

521 **References**

- 522 Augusti, A., Betson, T. R. and Schleucher, J.: Hydrogen exchange during cellulose
523 synthesis distinguishes climatic and biochemical isotope fractionations in tree rings,
524 *New Phytol.*, 172, 490–499, doi:10.1111/j.1469-8137.2006.01843.x, 2006.
- 525 Augusti, A. and Schleucher, J.: The ins and outs of stable isotopes in plants, *New*
526 *Phytol.*, 174, 473–475, doi:10.1111/j.1469-8137.2007.02075.x, 2007.
- 527 Badeck, F.-W., Tcherkez, G., Nogués, S., Piel, C. and Ghashghaie, J.: Post-
528 photosynthetic fractionation of stable carbon isotopes between plant organs - a
529 widespread phenomenon, *Rapid Commun. Mass Spectrom.*, 19, 1381–1391,
530 doi:10.1002/rcm.1912, 2005.
- 531 Barbour, M. M.: Stable oxygen isotope composition of plant tissue: a review, *Funct.*
532 *Plant Biol.*, 34, 83–94, doi:10.1071/FP06228, 2007.
- 533 Bird, J. A. and Torn, M. S.: Fine roots vs. needles: a comparison of ^{13}C and ^{15}N
534 dynamics in a ponderosa pine forest soil, *Biogeochemistry*, 79, 361–382,
535 doi:10.1007/s10533-005-5632-y, 2006.
- 536 Bowling, D. R., Pataki, D. E. and Randerson, J. T.: Carbon isotopes in terrestrial
537 ecosystem pools and CO_2 fluxes, *New Phytol.*, 178, 24–40, doi:10.1111/j.1469-
538 8137.2007.02342.x, 2008.

539 Cappa, C. D., Hendricks, M. B., Depaolo, D. J. and Cohen, R. C.: Isotopic
540 fractionation of water during evaporation, *J. Geophys. Res.*, 108, 4525,
541 doi:10.1029/2003JD003597, 2003.

542 Coplen, T. B.: Guidelines and recommended terms for expression of stable-isotope-
543 ratio and gas-ratio measurement results, *Rapid Commun. Mass Spectrom.*, 25,
544 2538–2560, doi:10.1002/rcm.5129, 2011.

545 Craig, H. and Gordon, L. I.: Deuterium and oxygen 18 variations in the ocean and the
546 marine atmosphere, in *Stable isotopes in oceanographic studies and*
547 *paleotemperatures*, edited by E. Tongiorgi, pp. 9–130, Spoleto, Pisa, Italy., 1965.

548 Dawson, T. E., Mambelli, S., Plamboeck, A. H., Templer, P. H. and Tu, K. P.: Stable
549 isotopes in plant ecology, *Annu. Rev. Ecol. Syst.*, 33, 507–559,
550 doi:10.1146/annurev.ecolsys.33.020602.095451, 2002.

551 Dongmann, G., Nürnberg, H. W., Förstel, H. and Wagener, K.: On the enrichment of
552 H_2^{18}O in the leaves of transpiring plants, *Radiat. Environ. Biophys.*, 11, 41–52,
553 doi:10.1007/BF01323099, 1974.

554 Farquhar, G. D. and Cernusak, L. A.: On the isotopic composition of leaf water in the
555 non-steady state, *Funct. Plant Biol.*, 32, 293–303, doi:10.1071/FP04232, 2005.

556 Farquhar, G. D. and Lloyd, J.: Carbon and oxygen isotope effects in the exchange of
557 CO_2 between terrestrial plants and the atmosphere, in *Stable isotopes and plant*
558 *carbon-water relations*, edited by J. R. Ehleringer, A. E. Hall, and G. D. Farquhar,
559 pp. 47–70, Academic Press, Waltham., 1993.

560 Filot, M.: *Isotopes in tree-rings: Development and application of a rapid preparative*
561 *online equilibration method for the determination of D / H ratios of*
562 *nonexchangeable hydrogen in tree-ring cellulose*, 106 pp., Bern., 2010.

563 Filot, M. S., Leuenberger, M., Pazdur, A. and Boettger, T.: Rapid online equilibration
564 method to determine the D/H ratios of non-exchangeable hydrogen in cellulose,
565 *Rapid Commun. Mass Spectrom.*, 20, 3337–3344, doi:10.1002/rcm, 2006.

566 Garcia-Martin, M. L., Ballesteros, P. and Cerda, S.: The metabolism of water in cells
567 and tissues as detected by NMR methods, *Prog. Nucl. Magn. Reson. Spectrosc.*, 39,
568 41–77, doi:10.1016/S0079-6565(01)00031-0, 2001.

569 Gehre, M., Geilmann, H., Richter, J., Werner, R. A. and Brand, W. A.: Continuous
570 flow $^2\text{H}/^1\text{H}$ and $^{18}\text{O}/^{16}\text{O}$ analysis of water samples with dual inlet precision, *Rapid*
571 *Commun. Mass Spectrom.*, 18, 2650–2660, doi:10.1002/rcm.1672, 2004.

572 Gessler, A., Brandes, E., Keitel, C., Boda, S., Kayler, Z. E., Granier, A., Barbour, M.,
573 Farquhar, G. D. and Treydte, K.: The oxygen isotope enrichment of leaf-exported
574 assimilates - does it always reflect lamina leaf water enrichment?, *New Phytol.*, 200,
575 144–157, doi:10.1111/nph.12359, 2013.

576 Girardin, C., Rasse, D. P., Biron, P., Ghashghaie, J. and Chenu, C.: A method for ¹³C-
577 labeling of metabolic carbohydrates within French bean leaves (*Phaseolus vulgaris*
578 L.) for decomposition studies in soils, *Rapid Commun. Mass Spectrom.*, 23, 1792–
579 1800, doi:10.1002/rcm, 2009.

580 Goldsmith, G. R.: Changing directions : the atmosphere-plant-soil continuum, *New*
581 *Phytol.*, 199, 4–6, 2013.

582 Hangartner, S., Kress, A., Saurer, M., Frank, D. and Leuenberger, M.: Methods to
583 merge overlapping tree-ring isotope series to generate multi-centennial
584 chronologies, *Chem. Geol.*, 294, 127–134, doi:10.1016/j.chemgeo.2011.11.032,
585 2012.

586 Högberg, P., Högberg, M. N., Göttlicher, S. G., Betson, N. R., Keel, S. G., Metcalfe,
587 D. B., Campbell, C., Schindlbacher, A., Hurry, V., Lundmark, T., Linder, S. and
588 Näsholm, T.: High temporal resolution tracing of photosynthate carbon from the tree
589 canopy to forest soil microorganisms, *New Phytol.*, 177, 220–228,
590 doi:10.1111/j.1469-8137.2007.02238.x, 2008.

591 Keel, S. G., Siegwolf, R. T. W. and Körner, C.: Canopy CO₂ enrichment permits
592 tracing the fate of recently assimilated carbon in a mature deciduous forest, *New*
593 *Phytol.*, 172, 319–329, doi:10.1111/j.1469-8137.2006.01831.x, 2006.

594 Kim, S., Kramer, R. W. and Hatcher, P. G.: Graphical method for analysis of
595 ultrahigh-resolution broadband mass spectra of natural organic matter, the van
596 Krevelen diagram, *Anal. Chem.*, 75, 5336–5344, doi:10.1021/ac034415p, 2003.

597 Kulmatiski, A., Beard, K. H., Verweij, R. J. T. and February, E. C.: A depth-
598 controlled tracer technique measures vertical, horizontal and temporal patterns of
599 water use by trees and grasses in a subtropical savanna, *New Phytol.*, 188, 199–209,
600 doi:10.1111/j.1469-8137.2010.03338.x, 2010.

601 Majoube, M.: Fractionnement en oxygène 18 et en deutérium entre l'eau et sa vapeur,
602 *J. Chim. Phys. physico-chimie Biol.*, 68, 1423–1435, 1971.

603 Meinzer, F. C., Hinckley, T. M. and Ceulemans, R.: Apparent responses of stomata to
604 transpiration and humidity in a hybrid poplar canopy, *Plant, Cell Environ.*, 20,
605 1301–1308, doi:10.1046/j.1365-3040.1997.d01-18.x, 1997.

606 Offermann, C., Ferrio, J. P., Holst, J., Grote, R., Siegwolf, R. T. W., Kayler, Z. E. and
607 Gessler, A.: The long way down-are carbon and oxygen isotope signals in the tree
608 ring uncoupled from canopy physiological processes?, *Tree Physiol.*, 31, 1088–
609 1102, doi:10.1093/treephys/tpr093, 2011.

610 Ohno, T., He, Z., Sleighter, R. L., Honeycutt, C. W. and Hatcher, P. G.: Ultrahigh
611 resolution mass spectrometry and indicator species analysis to identify marker
612 components of soil- and plant biomass- derived organic matter fractions, *Environ.*
613 *Sci. Technol.*, 44, 8594–8600, doi:10.1021/es101089t, 2010.

614 Parkhurst, D. F.: Tansley review no. 65. Diffusion of CO₂ and other gases inside
615 leaves, *New Phytol.*, 126, 449–479, doi:10.1111/j.1469-8137.1994.tb04244.x, 1994.

616 Plamboeck, A. H., Dawson, T. E., Egerton-Warburton, L. M., North, M., Bruns, T. D.
617 and Querejeta, J. I.: Water transfer via ectomycorrhizal fungal hyphae to conifer
618 seedlings, *Mycorrhiza*, 17, 439–447, doi:10.1007/s00572-007-0119-4, 2007.

619 Reynolds Henne, C. E.: A study of leaf water $\delta^{18}\text{O}$ composition using isotopically-
620 depleted H₂¹⁸O-vapour, in *Climate-isotope relationships in trees under non-limiting*
621 *climatic conditions from seasonal to century scales*, pp. 77–92, University of Bern.,
622 2007.

623 Rinne, K. T., Saurer, M., Streit, K. and Siegwolf, R. T. W.: Evaluation of a liquid
624 chromatography method for compound-specific $\delta^{13}\text{C}$ analysis of plant carbohydrates
625 in alkaline media, *Rapid Commun. Mass Spectrom.*, 26, 2173–85,
626 doi:10.1002/rcm.6334, 2012.

627 Roden, J. S. and Ehleringer, J. R.: Hydrogen and oxygen isotope ratios of tree-ring
628 cellulose for riparian trees grown long-term under hydroponically controlled
629 environments, *Oecologia*, 121, 467–477, doi:10.1007/s004420050953, 1999.

630 Roden, J. S. and Farquhar, G. D.: A controlled test of the dual-isotope approach for
631 the interpretation of stable carbon and oxygen isotope ratio variation in tree rings,
632 *Tree Physiol.*, 32, 1–14, doi:10.1093/treephys/tps019, 2012.

633 Scheidegger, Y., Saurer, M., Bahn, M. and Siegwolf, R. T. W.: Linking stable oxygen
634 and carbon isotopes with stomatal conductance and photosynthetic capacity: A
635 conceptual model, *Oecologia*, 125, 350–357, doi:10.1007/S004420000466, 2000.

636 Schenck zu Schweinsberg-Mickan, M., Joergensen, R. G. and Müller, T.: Fate of ¹³C-
637 and ¹⁵N-labelled rhizodeposition of *Lolium perenne* as function of the distance to the
638 root surface, *Soil Biol. Biochem.*, 42, 910–918, doi:10.1016/j.soilbio.2010.02.007,
639 2010.

640 Schmidt, H.-L., Werner, R. A. and Eisenreich, W.: Systematics of ^2H patterns in
641 natural compounds and its importance for the elucidation of biosynthetic pathways,
642 *Phytochem. Rev.*, 2, 61–85, doi:10.1023/B:PHYT.0000004185.92648.ae, 2003.

643 Schmidt, H.-L., Werner, R. A. and Rossmann, A.: O-18 pattern and biosynthesis of
644 natural plant products, *Phytochemistry*, 58, 9–32, doi:10.1016/S0031-
645 9422(01)00017-6, 2001.

646 Simard, S. W., Durall, D. M. and Jones, M. D.: Carbon allocation and carbon transfer
647 between *Betula papyrifera* and *Pseudotsuga menziesii* seedlings using a ^{13}C pulse-
648 labeling method, *Plant Soil*, 191, 41–55, doi:10.1023/A:1004205727882, 1997.

649 Sleighter, R. L. and Hatcher, P. G.: The application of electrospray ionization coupled
650 to ultrahigh resolution mass spectrometry for the molecular characterization of
651 natural organic matter, *J. Massspectrometry*, 42, 559–574, doi:10.1002/jms, 2007.

652 Steinmann, K., Siegwolf, R. T. W., Saurer, M. and Körner, C.: Carbon fluxes to the
653 soil in a mature temperate forest assessed by ^{13}C isotope tracing, *Oecologia*, 141,
654 489–501, doi:10.1007/s00442-004-, 2004.

655 Sternberg, L. D. S. L. O., DeNiro, M. J. D. and Savidge, R. A.: Oxygen isotope
656 exchange between metabolites and water during biochemical reactions leading to
657 cellulose synthesis, *Plant Physiol.*, 82, 423–427, doi:10.1104/pp.82.2.423, 1986.

658 Studer, M. S., Siegwolf, R. T. W. and Abiven, S.: Carbon transfer, partitioning and
659 residence time in the plant-soil system: a comparison of two $^{13}\text{CO}_2$ labelling
660 techniques, *Biogeosciences*, 11, 1637–1648, doi:10.5194/bg-11-1637-2014, 2014.

661 Werner, C., Schnyder, H., Cuntz, M., Keitel, C., Zeeman, M. J., Dawson, T. E.,
662 Badeck, F.-W., Brugnoli, E., Ghashghaie, J., Grams, T. E. E., Kayler, Z. E., Lakatos,
663 M., Lee, X., Máguas, C., Ogée, J., Rascher, K. G., Siegwolf, R. T. W., Unger, S.,
664 Welker, J., Wingate, L. and Gessler, A.: Progress and challenges in using stable
665 isotopes to trace plant carbon and water relations across scales, *Biogeosciences*, 9,
666 3083–3111, doi:10.5194/bg-9-3083-2012, 2012.

667 Yakir, D. and DeNiro, M. J. D.: Oxygen and hydrogen isotope fractionation during
668 cellulose metabolism in *Lemna gibba* L., *Plant Physiol.*, 93, 325–332,
669 doi:10.1104/pp.93.1.325, 1990.

670 Zech, M., Saurer, M., Tuthorn, M., Rinne, K., Werner, R. a, Siegwolf, R., Glaser, B.
671 and Juchelka, D.: A novel methodological approach for $\delta(18)\text{O}$ analysis of sugars
672 using gas chromatography-pyrolysis-isotope ratio mass spectrometry., *Isotopes*
673 *Environ. Health Stud.*, 49, 492–502, doi:10.1080/10256016.2013.824875, 2013.

674
675

675 **Tables**

676 **Table 1.** Diffusion of atmospheric water vapour into the leaf water. $\delta^{18}\text{O}$ and $\delta^2\text{H}$
677 signatures of leaf water and its two sources: i) the evaporating source (Eq. 3),
678 estimated by the stem water signature plus kinetic and equilibrium leaf water
679 enrichment (assuming full evaporation without back-diffusion), and ii) the
680 condensation source (Eq. 4), assessed by the atmospheric water vapour signature plus
681 equilibrium fractionation to account for the gas-liquid phase change. The contribution
682 of the second source (diffusion and condensation of atmospheric water vapour) to the
683 leaf water ($f_{\text{source},2/\text{leaf},\text{water}}$) was estimated by a two-source isotope mixing model for
684 ^{18}O and ^2H separately (Eq. 2). Presented are the average values of three plant
685 replicates for each sampling date \pm one standard deviation

Sampling date (days)	Leaf water ⁽¹⁾		Source 1: Evaporating source ⁽²⁾		Source 2: Condensation source ⁽²⁾		$f_{\text{source},2/\text{leaf},\text{water}}$ ⁽²⁾	
	$\delta^{18}\text{O}$ (‰)	$\delta^2\text{H}$ (‰)	$\delta^{18}\text{O}$ (‰)	$\delta^2\text{H}$ (‰)	$\delta^{18}\text{O}$ (‰)	$\delta^2\text{H}$ (‰)	^{18}O (%)	^2H (%)
0	-1.0 (± 0.5)	-32.0 (± 1.8)	21.3 (± 0.4)	10.9 (± 2.6)	-8.8	-99.7	74.2 (± 1.2)	38.8 (± 0.3)
1	-11.7 (± 1.8)	-53.0 (± 5.9)	19.5 (± 0.3)	10.3 (± 3.2)	-27.3	-143.3	66.6 (± 3.9)	41.2 (± 3.2)
2	-65.6 (± 6.5)	-162.3 (± 8.6)	20.0 (± 0.6)	14.4 (± 2.1)	-47.6	-196.0	126.6 (± 9.8)	84.0 (± 4.1)
8	-65.2 (± 2.0)	-159.9 (± 3.8)	20.0 (± 0.7)	5.3 (± 3.9)	-98.6	-274.8	71.8 (± 1.5)	59.0 (± 0.8)
14	-60.4 (± 10.7)	-152.3 (± 21.2)	19.3 (± 0.4)	9.5 (± 5.1)	-101.8	-275.8	65.8 (± 8.7)	56.8 (± 6.8)

⁽¹⁾ directly measured

⁽²⁾ calculated

686

686 **Table 2.** Multi-isotope labelling of bulk organic matter. $\delta^{13}\text{C}$, $\delta^{18}\text{O}$ and $\delta^2\text{H}$ signatures
687 (in ‰) of the plant-soil compartments (three replicates \pm one standard deviation)
688 measured before and after 1, 2, 8 and 14 days of continuous labelling. A significant
689 enrichment ($\delta^{13}\text{C}$) and depletion ($\delta^{18}\text{O}$, $\delta^2\text{H}$) compared to the unlabelled control (t =
690 0) is highlighted with * (t-test, P < 0.05). The degree of labelling is indicated by the
691 change in the isotopic signature of the last sampling date (t = 14) compared to the
692 control

Sampling date (days)						
$\delta^{13}\text{C}$ (‰)	0	1	2	8	14	14 - 0 ⁽¹⁾
Leaves	-30.8 (± 0.4)	161.5* (± 37.4)	189.7 (± 128.7)	570.7* (± 81.0)	812.5* (± 235.0)	843.3 ± 235.0
Petioles	-32.8 (± 0.2)	163.9* (± 56.2)	212.8* (± 75.2)	908.5* (± 277.3)	941.9* (± 292.7)	974.7 (± 292.7)
Stems	-31.4 (± 0.6)	209.6* (± 84.2)	281.3* (± 87.6)	1093.7* (± 402.2)	1119.9* (± 367.6)	1151.3 (± 367.6)
Cuttings	-31.2 (± 0.3)	-27.0* (± 1.6)	-26.9 (± 1.9)	-14.6 (± 15.8)	-14.5* (± 2.1)	16.8 (± 2.1)
Roots	-30.8 (± 0.7)	98.1* (± 12.5)	90.8 (± 62.9)	646.5 (± 335.1)	618.0* (± 310.9)	648.8 (± 310.9)
Bulk soil	-28.0 (± 0.1)	-27.9 (± 0.0)	-27.8 (± 0.2)	-27.5 (± 0.5)	-27.5 (± 0.2)	0.5 (± 0.3)
$\delta^{18}\text{O}$ (‰)	0	1	2	8	14	14 - 0 ⁽¹⁾
Leaves	25.9 (± 0.8)	25.2 (± 0.8)	21.9 (± 2.0)	15.0* (± 0.4)	9.0* (± 3.0)	-16.9 (± 3.2)
Petioles	21.0 (± 0.2)	20.4 (± 0.4)	19.5* (± 0.4)	14.3* (± 1.6)	12.8* (± 2.3)	-8.2 (± 2.3)
Stems	22.4 (± 0.4)	22.2 (± 0.1)	20.6* (± 0.8)	14.7* (± 2.4)	13.3* (± 2.8)	-9.1 (± 2.8)
Cuttings	21.3 (± 1.5)	21.9 (± 0.1)	21.8 (± 0.4)	21.5 (± 0.3)	21.5 (± 0.4)	0.2 (± 1.5)
Roots	21.2 (± 0.6)	20.6 (± 0.6)	20.9 (± 0.4)	18.2 (± 1.5)	17.5* (± 1.7)	-3.7 (± 1.8)
Bulk soil	14.8 (± 0.4)	14.0 (± 0.3)	13.8* (± 0.4)	13.0* (± 0.1)	13.5 (± 0.8)	-1.3 (± 0.9)
$\delta^2\text{H}$ (‰)	0	1	2	8	14	14 - 0 ⁽¹⁾
Leaves	-146.6 (± 2.5)		-158.1 (± 7.8)	-169.2* (± 5.5)	-178.0* (± 9.4)	-31.3 (± 9.7)
Petioles	-138.3 (± 1.8)				-150.9 (± 6.7)	-12.6 (± 7.3)
Stems	-129.2 (± 4.2)		-136.3 (± 4.7)	-153.3 (± 14.8)	-152.9* (± 9.4)	-23.7 (± 10.3)
Cuttings	-167.3 (± 2.8)				-172.8 (± 6.3)	-5.5 (± 6.9)
Roots	-129.7 (± 6.4)		-134.0 (± 12.5)	-137.0 (± 6.8)	-135.9 (± 7.7)	-6.2 (± 10.0)
Bulk soil	-101.5 (± 1.1)				-101.9 (± 1.3)	0.4 (± 1.7)

⁽¹⁾ Isotopic difference for the entire labelling experiment

693 **Table 3.** Atomic and isotopic ratios of the labelled bulk organic matter. C/N, O/C and
 694 H/C atomic ratios and $^{18}\text{O}/^{13}\text{C}$ and $^2\text{H}/^{13}\text{C}$ isotopic ratios (of the excess atom fraction)
 695 measured in different plant compartments after the equilibrium in the atmospheric
 696 labelling was reached. Indicated are average values of two sampling dates (t = 8 and
 697 14) with three plant replicates each (\pm one standard deviation)

Compartment	C/N	O/C	H/C	$^{18}\text{O}/^{13}\text{C}^{(1)}$	$^2\text{H}/^{13}\text{C}^{(1)}$
Leaves	13.7 (± 0.4)	0.70 (± 0.01)	1.72 (± 0.04)	0.43 (± 0.07)	0.41 (± 0.06)
Petioles	35.4 (± 1.3)	0.77 (± 0.01)	1.64 (± 0.01)	0.18 (± 0.03)	0.14 (± 0.03) ⁽²⁾
Stems	32.0 (± 4.0)	0.83 (± 0.01)	1.71 (± 0.02)	0.17 (± 0.03)	0.23 (± 0.06)
Cuttings	115.4 (± 7.2)	0.72 (± 0.01)	1.56 (± 0.02)	n.c. ⁽³⁾	n.c. ⁽³⁾
Roots	29.9 (± 2.0)	0.73 (± 0.02)	1.61 (± 0.02)	0.12 (± 0.03)	0.07 (± 0.11)

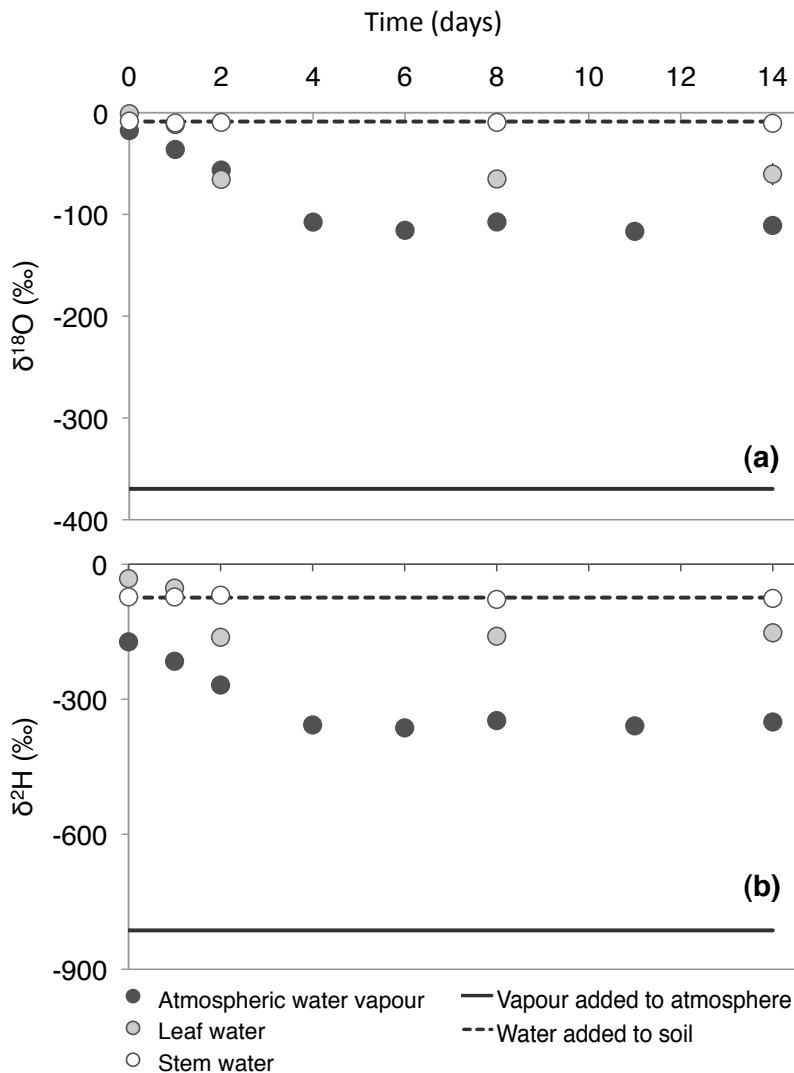
⁽¹⁾ Ratio of excess atom fraction normalized by the maximum label strength (Eq. 7)

⁽²⁾ Only the last sampling date was measured (t = 14)

⁽³⁾ Not calculated (no consistent ^{18}O and ^2H depletion detected in the tissue)

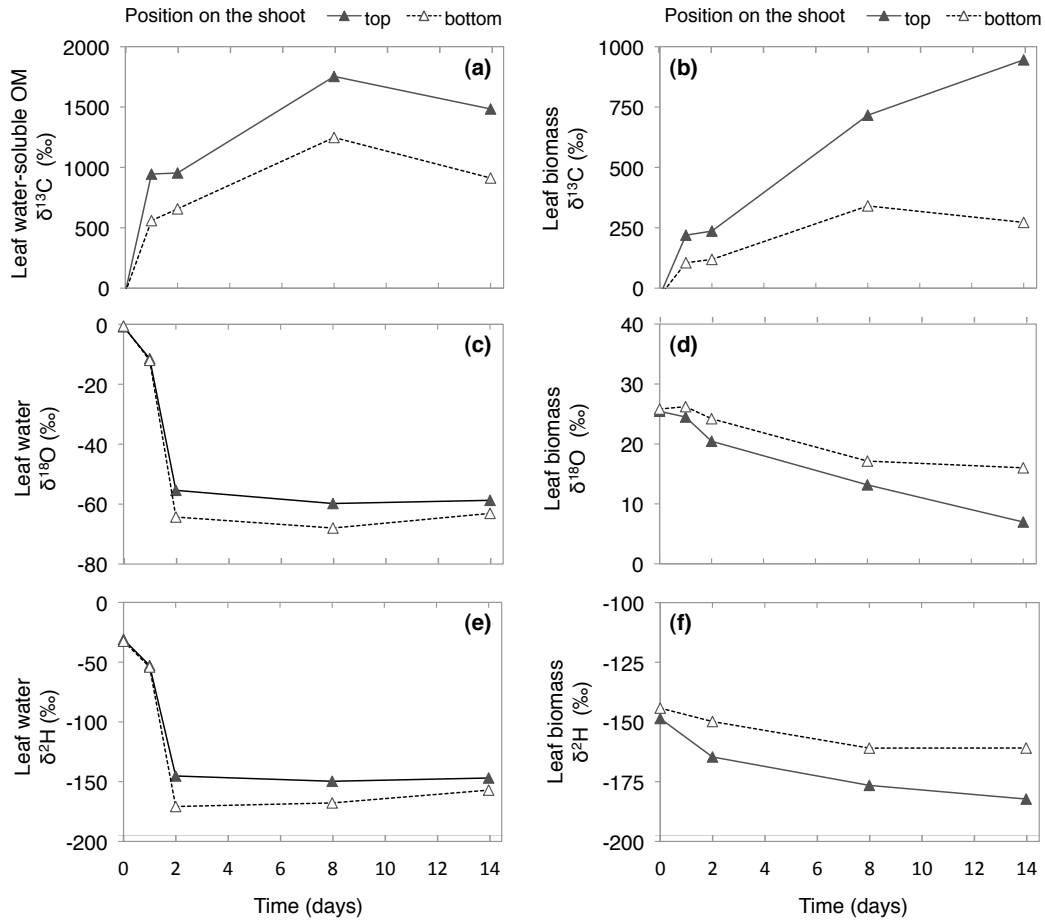
698

698 **Figures**

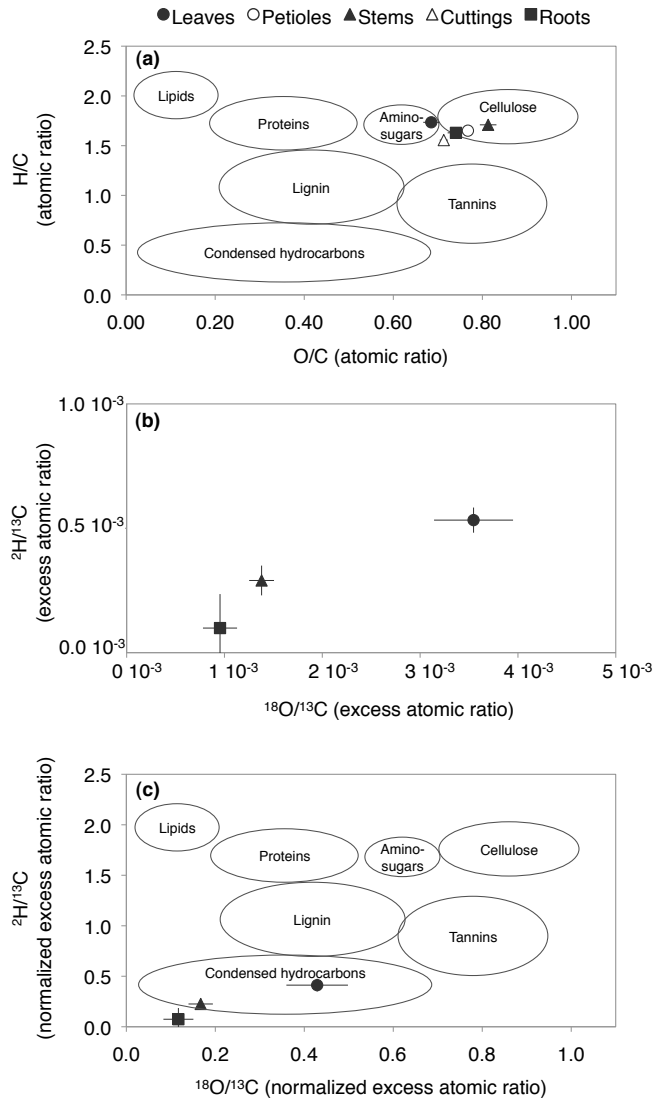


699

700 **Figure 1.** Temporal dynamics in the water isotopic signatures of the plant-soil-
 701 atmosphere system during continuous $^2\text{H}_2^{18}\text{O}$ labelling (a) $\delta^{18}\text{O}$ and (b) $\delta^2\text{H}$ signature
 702 (in ‰) of the depleted water label added as water vapour to the atmosphere (solid
 703 line), of the water added to the soil (dashed line), of the resulting water vapour in the
 704 chamber atmosphere (black dots) and of the extracted leaf (grey dots) and stem water
 705 (white dots). Error bars on the leaf water indicate \pm one standard deviation of three
 706 plant replicates

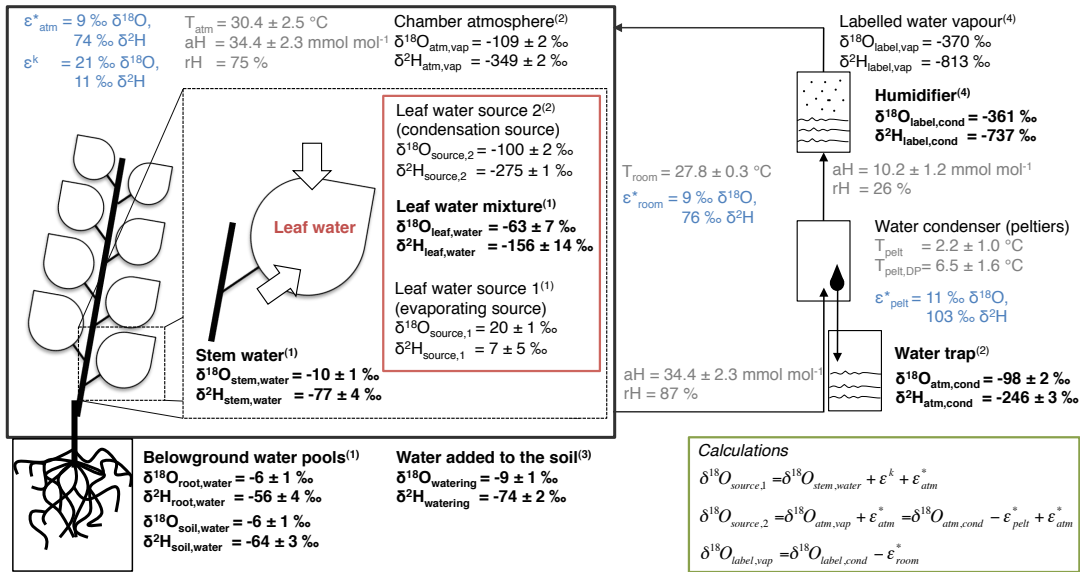


707
 708 **Figure 2.** Incorporation of the gaseous labels ($^{13}\text{CO}_2$, $^2\text{H}_2^{18}\text{O}$) into the leaf water
 709 water-soluble and bulk organic matter. (a,b) $\delta^{13}\text{C}$, (c,d) $\delta^{18}\text{O}$ and (e,f) $\delta^2\text{H}$ signature
 710 (in ‰) within leaves sampled at the top (solid line, black triangles), or at the bottom
 711 (dashed line, white triangles) of the shoot. Illustrated are the signatures of (a) the leaf
 712 water-soluble organic matter, (b,e,f) the leaf biomass and (c,e) the leaf water



713

714 **Figure 3.** Atomic and isotopic ratios to illustrate change in organic matter
 715 characteristics (a) Atomic and (b,c) isotopic ratios of oxygen and hydrogen to carbon
 716 within the leaves (closed circles), petioles (open circles), stems (closed triangle), stem
 717 cutting (open triangle) and roots (closed square). The circles overlain on the plots in
 718 (a) and (c) indicate atomic ratios characteristic for different compound classes
 719 (adapted from Sleighter & Hatcher, 2007). (a) illustrates the atomic ratio of all tissues
 720 measured (15 replicates \pm one standard deviation, (b) the isotopic ratios of the ^{13}C ,
 721 ^{18}O and ^2H excess atom fraction (relative to the unlabelled tissues) measured after
 722 equilibrium in the labelling (see Fig. 1 and 2) was reached ($t = 8$ and 14, six replicates
 723 \pm one standard deviation) and (c) shows the isotopic ratios of after normalization with
 724 the maximum label strength of the leaf water (^{18}O , ^2H) and water-soluble organic
 725 matter (^{13}C)



(1) Sampled after 3/12 hours daylight; errors represent variability between plant individuals (three plant replicates each sampling date).
 (2) Integrated value over 2-3 days (water trap analysed at day 6, 8, 11 and 14), errors represent variability between sampling date 8 and 14.
 (3) Average of all watering dates (day 0, 2, 6, 8, 11); errors represent variability between sampling dates.
 (4) Measured at the beginning of the experiment

727
 728 **Figure A1.** Overview on the input data of the two-source isotope mixing model. $\delta^{18}\text{O}$
 729 and $\delta^2\text{H}$ signatures of the water pools of the chamber system are presented as average
 730 values after equilibrium in the labelling was reached ($t = 8$ and 14 days). The
 731 monitored environmental conditions ($T =$ temperature, $a\text{H} =$ absolute humidity and $r\text{H} =$
 732 relative humidity) are presented in grey. The equilibrium and kinetic fractionation
 733 factors, highlighted in blue, were calculated according to Majoube (1971) and Cappa
 734 et al. (2003), respectively. The fractionation factors were used for the calculations
 735 (green box) of the signatures in the non-directly measured pools and the isotopic
 736 signatures of the evaporating and condensation source of the leaf water (red box). The
 737 equations are given for $\delta^{18}\text{O}$, but apply for $\delta^2\text{H}$ analogously. Please note that the data
 738 reported here are average values of the two last sampling dates, while we present in
 739 the result section the data of single sampling dates or average values of the whole
 740 labelling experiment (environmental conditions, equilibrium fractionation factors)

741 **Appendix B**

742 Calculation of the relative air humidity and the dew-point temperature

743 The dew-point temperature, i.e. the temperature at which the water condensed inside
 744 the peltier-cooled water condenser ($T_{\text{pelt,DP}}$) was calculated by solving Equation B1
 745 with the humidity measured in the air after the condenser ($10 \pm 1 \text{ mmol mol}^{-1}$ aH, 26
 746 % rH).

747
$$rH(T) = \frac{e}{e(T)} \cdot 100 \tag{B1}$$

748 , where rH is the relative air humidity (in %), e is the partial pressure of water vapour
749 (calculated according to Eq. B2) and e(T) is the saturation vapour pressure (in kPa,
750 calculated according to Eq. B3).

751
$$e = \frac{aH}{1000} \cdot p \tag{B2}$$

752 , where aH is the absolute humidity given as the mole fraction of water vapour (mmol
753 mol⁻¹) and p is the atmospheric pressure (in kPa).

754
$$e(T) = 0.61365 \cdot e^{\frac{17.502 \cdot T}{240.97 + T}} \tag{B3}$$

755 , where T is the room air temperature (in °C).

756 References

757 Cappa C.D., Hendricks M.B., Depaolo D.J. and Cohen R.C.: Isotopic fractionation of
758 water during evaporation. *J Geophys. Res.*, 108,: 4525. doi: 10.1029/2003
759 JD003597, 2003.

760 Majoube M.: Fractionnement en oxygène 18 et en deutérium entre l'eau et sa vapeur.
761 *J. Chim. Phys. physico-chimie Biol.*, 68,1423–1435. 1971.